

MLH1, PMS1, and MSH2 Interactions During the Initiation of DNA Mismatch Repair in Yeast

Tomas A. Prolla,* Qishen Pang,* Eric Alani, Richard D. Kolodner, R. Michael Liskay†

The discovery that mutations in DNA mismatch repair genes can cause hereditary non-polyposis colorectal cancer has stimulated interest in understanding the mechanism of DNA mismatch repair in eukaryotes. In the yeast *Saccharomyces cerevisiae*, DNA mismatch repair requires the MSH2, MLH1, and PMS1 proteins. Experiments revealed that the yeast MLH1 and PMS1 proteins physically associate, possibly forming a heterodimer, and that MLH1 and PMS1 act in concert to bind a MSH2-heteroduplex complex containing a G-T mismatch. Thus, MSH2, MLH1, and PMS1 are likely to form a ternary complex during the initiation of eukaryotic DNA mismatch repair.

Hereditary nonpolyposis colorectal cancer (HNPCC) is a common cancer predisposition syndrome characterized by early onset of carcinomas of the colon, as well as cancers of the endometrium, stomach, upper urinary tract, small intestine, and ovary (1). Inherited mutations in two DNA mismatch repair gene homologs, *hMSH2* and *hMLH1*, account for much of HNPCC (2–5). At the molecular level, HNPCC tumors are characterized by an increase in mutation rate within microsatellite sequences (6, 7). A colon cancer cell line that is defective in DNA mismatch repair and homozygous for an *hMLH1* mutation (3) was found to display not only increased microsatellite instability, but also a general increase in the rate of spontaneous mutation (8, 9). Additionally, both *hMSH2* alleles were found to be mutated in a tumor with microsatellite instability obtained from an individual with HNPCC (5). The observation that 10 to 45% of pancreatic, gastric, breast, ovarian, and small-cell lung cancers display microsatellite instability (10) suggests that defective DNA mismatch repair is not restricted to HNPCC tumors but is a common feature in tumor initiation or progression. The precise role of the *hMSH2* and *hMLH1* proteins in DNA mismatch repair is currently unknown.

Genetic studies have demonstrated that the major DNA mismatch repair pathway in *S. cerevisiae* requires a bacterial MutS homolog, MSH2 (11, 12), and two bacterial MutL homologs, MLH1 and PMS1 (13,

14). On the basis of these genetic studies (11–15) and the observation that bacterial MutL exists as a homodimer in solution and interacts with MutS in the presence of heteroduplex DNA (16), we tested physical interactions between yeast MLH1, PMS1, and MSH2.

We initially used the yeast two-hybrid system (17) to study in vivo interactions between MLH1, PMS1, and MSH2. These proteins were fused to the LexA and GAD proteins, and pairwise combinations were tested for their ability to induce β -galactosidase activity in the appropriate *S. cerevisiae* host (18, 19). Of all the combinations tested (GAD-MLH1 with LexA-PMS1; GAD-MLH1 with LexA-MLH1; GAD-PMS1 with LexA-PMS1; GAD-MSH2 with LexA-PMS1; GAD-MSH2 with LexA-MLH1; GAD with LexA; and GAD with LexA-PMS1), only the GAD-MLH1–LexA-PMS1 pair induced β -galactosidase activity, suggesting that these two proteins physically associate.

We then used maltose binding protein (MBP) affinity chromatography (20) to

study associations between MLH1, PMS1, and MSH2 in vitro. Each of these proteins was prepared as an MBP fusion protein, immobilized on an amylose resin, and tested for binding to PMS1, MLH1, and MSH2, synthesized in vitro (Fig. 1A). PMS1 bound efficiently to an MBP-MLH1 matrix (Fig. 1B) but weakly to an MBP-PMS1 matrix (Fig. 1C). Conversely, MLH1 bound efficiently to an MBP-PMS1 matrix (Fig. 1C) but did not bind to an MBP-MLH1 matrix (Fig. 1B). MSH2 showed no substantial binding to any of the affinity matrices. MLH1 alone, PMS1 alone, or the combination of these proteins bound only weakly to an MBP-MSH2 matrix (21). Therefore, neither protein displays strong affinity for MSH2 under these conditions. From the affinity chromatography and yeast two-hybrid results, we conclude that MLH1 and PMS1 associate and are likely to form a heterodimer, or higher order multimer.

To determine whether MLH1 and PMS1 proteins interact with MSH2 bound to heteroduplex DNA, we constructed 108-bp homoduplexes and heteroduplexes containing a G-T mismatch and used a gel retardation assay to analyze the DNA binding properties of MSH2, MLH1, and PMS1 overproduced in *Escherichia coli* (22). Densitometer scans of gel retardation autoradiograms indicated that the MSH2 binding affinity for a G-T-containing heteroduplex was 10 to 20 times greater than that for the G-C-containing homoduplex (Fig. 2, lanes 2 and 8). A similar differential between the binding affinity of bacterial MutS to heteroduplexes and that to homoduplexes has been reported (23). Like bacterial MutL (24), the MLH1 and PMS1 proteins alone or in combination displayed similar, but low affinity for both homoduplexes and heteroduplexes (Fig. 2, lanes 3, 4, 9, 10, and 15).

In the presence of all three proteins, the characteristic MSH2-heteroduplex band shift

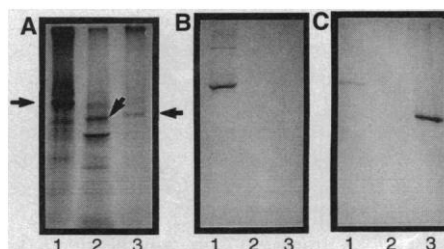


Fig. 1. In vitro interactions between MLH1, PMS1, and MSH2. MBP fusion proteins were synthesized in *E. coli* and bound to amylose resin as described (20). The *MSH2*, *MLH1*, and *PMS1* genes were cloned into pCite vectors (Novagen), which can be used for T7 RNA polymerase-directed transcription. Equal amounts of [35 S]methionine-labeled MSH2, MLH1, and PMS1, synthesized with the rabbit reticulocyte lysate system (Novagen), were individually passed through MBP matrix columns. Columns were washed with 10 volumes of buffer [20 mM Tris HCl (pH 7.4), 200 mM NaCl, and 1 mM EDTA], and the bound proteins were eluted with 2 ml of buffer plus 10 mM maltose and analyzed by SDS-PAGE. An identical amount of each affinity matrix eluate was used (10 μ l) for SDS-PAGE analysis. Gels were dried and subjected to autoradiography to visualize 35 S-labeled proteins. (A) In vitro-translated products, PMS1 (lane 1), MLH1 (lane 2), and MSH2 (lane 3). Arrows denote the expected full-length protein products as determined by comparison with molecular weight markers. (B) [35 S]methionine-labeled PMS1 (lane 1), MSH2 (lane 2), and MLH1 (lane 3) were individually passed through an MBP-MLH1 matrix and analyzed as described. (C) [35 S]methionine-labeled PMS1 (lane 1), MSH2 (lane 2), and MLH1 (lane 3) were individually passed through an MBP-PMS1 matrix and analyzed as described.

T. A. Prolla, Department of Molecular Biophysics and Biochemistry, Yale University School of Medicine, New Haven, CT 06511, USA, and Department of Molecular and Medical Genetics, Oregon Health Sciences University, Portland, OR 97201, USA.

Q. Pang and R. M. Liskay, Department of Molecular and Medical Genetics, Oregon Health Sciences University, Portland, OR 97201, USA.

E. Alani and R. D. Kolodner, Division of Cell and Molecular Biology, Dana Farber Cancer Institute and Department of Biological Chemistry and Molecular Pharmacology, Harvard Medical School, Boston, MA 02115, USA.

*These authors contributed equally to this work.

†To whom correspondence should be addressed.

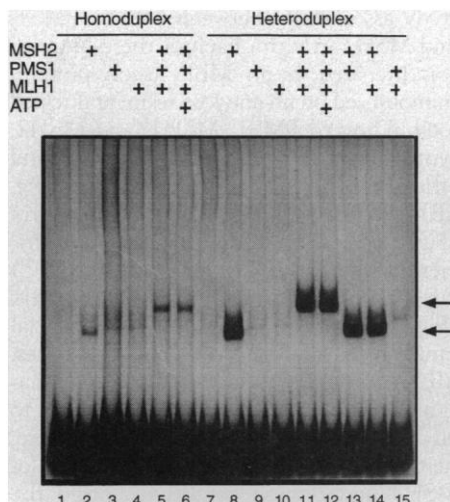
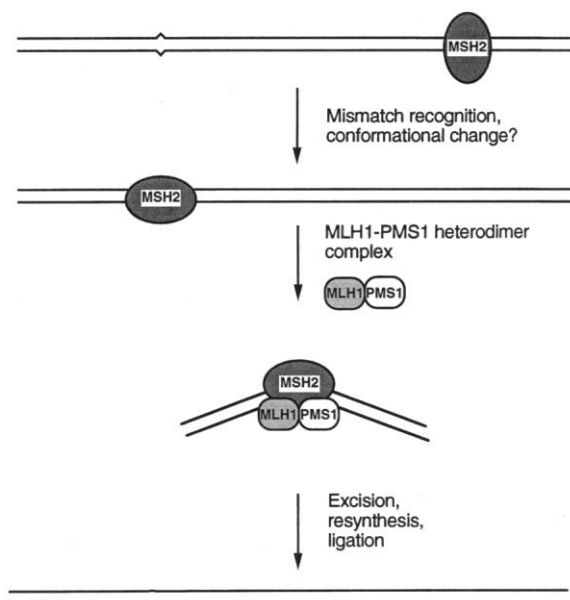


Fig. 2. Gel retardation assays. Binding reactions (20 μ l) contained 150 fmol of 32 P-labeled homoduplex or heteroduplex DNA (22), 1.5 mg of poly(deoxyinosine-deoxycytosine), 20 mM tris HCl (pH 7.6), 5 mM MgCl₂, 10 μ M EDTA, 100 μ M DTT, bovine serum albumin (200 mg/ml), and 12% glycerol. When present, the concentration of ATP was 0.1 mM. MSH2, MLH1, or PMS1 (10 pmol) were added (+) to the DNA in the indicated combinations. After incubation for 30 min at 0°C, the DNA species were resolved by electrophoresis through a 4% nondenaturing polyacrylamide gel at 4°C and then visualized by autoradiography. Bottom arrow denotes the MSH2-heteroduplex complex, and the top arrow denotes the ternary complex formed in the presence of heteroduplex, MSH2, MLH1, and PMS1.

was replaced by a lower mobility species indicative of a protein-DNA complex of higher molecular weight (Fig. 2, lane 11). Formation of this complex required the simultaneous presence of MLH1, PMS1, and MSH2 (Fig. 2, lane 11), did not require exogenous adenosine triphosphate (ATP) (Fig. 2, lanes 11 and 12), and occurred in the presence of either homoduplex or heteroduplex DNA, although to a greater extent with heteroduplex DNA (Fig. 2, lanes 5 and 11). Similar results were observed with MSH2 overproduced in *S. cerevisiae* (21). Although in other gel retardation studies MSH2 bound to 36-bp probes containing either a G-T mismatch or a 1-base deletion, the three proteins together did not form a higher molecular weight complex with this smaller DNA (21). Thus, a minimum DNA fragment size may be needed for ternary complex formation. The gel retardation results suggest that under our experimental conditions, MSH2 binding to DNA, rather than the presence of DNA mismatches, is a prerequisite for the formation of a ternary complex involving MSH2, MLH1, and PMS1.

Given the biochemical results described here and previous knowledge about the mechanism of bacterial DNA mismatch repair

Fig. 3. A model for early events in eukaryotic DNA mismatch repair. Eukaryotic DNA mismatch repair is initiated by MSH2 recognition of DNA single base pair mismatches or small heterologies, the latter presumed to occur as a result of strand misalignment during DNA replication of microsatellites. After recognition of a DNA mismatch, MSH2 may undergo a conformational change that increases its DNA binding affinity or alters the local DNA conformation, as has been proposed for bacterial MutS (16, 28). This is followed by binding of an MLH1-PMS1 heteromer to the MSH2-DNA complex, which in turn is likely to recruit additional proteins involved in actual repair. We favor a model in which productive interactions between the MLH1-PMS1 heteromer and MSH2 occur only in the presence of DNA mismatches. However, our gel retardation studies with homoduplex probes suggest that DNA-mediated interactions between the MLH1-PMS1 complex and MSH2 may occur after DNA binding but before mismatch recognition by MSH2. The stoichiometry of MSH2, MLH1, and PMS1 has not been established.



pair (25), we propose a model for the early events in eukaryotic DNA mismatch repair (Fig. 3). The binding of MSH2 to homoduplexes (Fig. 2) appears to be due to nonspecific affinity of MSH2 for DNA, which may be of physiological significance. Exploratory searches along DNA have been proposed to be one mechanism by which DNA binding proteins locate their specific recognition sites (26). Our results suggest that by binding to an MSH2-DNA mismatch complex, and perhaps by recruiting other proteins involved in repair, the MLH1-PMS1 pair may act as a "molecular matchmaker," as proposed for bacterial MutL by Sancar and Hearst (27). The formation of a ternary complex without exogenous ATP contrasts with the situation in bacteria, where MutL enhancement of the MutS-heteroduplex footprint is ATP-dependent (16). One explanation for this apparent discrepancy is that the ATP-dependent alteration of the MutS-heteroduplex footprint by MutL may reflect a step subsequent to the initial interaction between MutL and the MutS-DNA complex. Therefore, we suggest that the early steps of prokaryotic and eukaryotic DNA mismatch repair are mechanistically similar, despite the requirement for two MutL homologs in yeast. Finally, the observation that the yeast MLH1, PMS1, and MSH2 proteins form a ternary complex supports previous suggestions that at least one of the two recently identified human homologs of the yeast PMS1 gene is involved in HNPCC not associated with either hMSH2 or hMLH1 (2, 3).

Note added in proof: Recently, mutation of two human homologs of the yeast PMS1

gene has been associated with hereditary nonpolyposis colon cancer (29).

REFERENCES AND NOTES

1. H. T. Lynch *et al.*, *Gastroenterology* **104**, 1535 (1993); P. Watson and H. T. Lynch, *Cancer* **71**, 677 (1994).
2. C. E. Bronner *et al.*, *Nature* **368**, 258 (1994).
3. N. Papadopoulos *et al.*, *Science* **263**, 1625 (1994).
4. R. Fishel *et al.*, *Cell* **75**, 1027 (1993).
5. F. Leach *et al.*, *ibid.*, p. 1215.
6. L. A. Aaltonen *et al.*, *Science* **260**, 812 (1993).
7. A. Lindblom, P. Tannergård, B. Werelius, M. Nordenskjöld, *Nature Genet.* **5**, 279 (1993).
8. R. Parsons *et al.*, *Cell* **75**, 1227 (1993).
9. N. P. Bhattacharyya *et al.*, *Proc. Natl. Acad. Sci. U.S.A.* **91**, 6319 (1994).
10. Y. Ionov *et al.*, *Nature* **363**, 558 (1993); S. N. Thibodeau *et al.*, *Science* **260**, 816 (1993); H.-J. Han *et al.*, *Cancer Res.* **53**, 5087 (1993); J. I. Risinger *et al.*, *ibid.*, p. 5100; R. A. Loathe, *ibid.*, p. 5849; R. Wooster *et al.*, *Nature Genet.* **6**, 152 (1994); A. Merlo, *Cancer Res.* **54**, 2098 (1994).
11. R. A. Reenan and R. D. Kolodner, *Genetics* **132**, 975 (1992).
12. E. Alani, R. Reenan, R. D. Kolodner, *ibid.*, **137**, 19 (1994).
13. W. Kramer, B. Kramer, M. S. Williamson, S. Fogel, *J. Bacteriol.* **171**, 5339 (1989).
14. T. Prolla, D.-M. Christie, R. M. Liskay, *Mol. Cell. Biol.* **14**, 407 (1994).
15. M. Strand *et al.*, *Nature* **365**, 274 (1993).
16. M. Grilley, K. M. Welsh, S.-S. Su, P. Modrich, *J. Biol. Chem.* **264**, 1000 (1989).
17. S. Fields and O.-k. Song, *Nature* **340**, 245 (1989).
18. The MLH1, PMS1, and MSH2 genes were inserted into the cloning sites of plasmids pGAD (encoding GAL4 residues 768 to 881 and containing a yeast LEU2 gene as selectable marker) or pBTM (encoding the LexA DNA binding domain and containing the yeast TRP1 gene as a selectable marker) and were used to transform strains 801a or 801 α (*ade2 trp1-901 leu2-3, 112 his3-200 gal4 gal80 URA3::lexA op-lacZ*). We generated strains carrying the desired plasmid combinations by mating haploid strains containing pGAD or pBTM plasmids and selecting for diploids in media devoid of tryptophan and leucine. Individual colonies were patched onto selective media, transferred onto nitrocellulose filters, and grown

- overnight. Membranes were dropped into liquid nitrogen for 30 s, dried, and incubated at 30°C with the chromogenic substrate X-GAL [J. Breeden and K. Nasmyth, *Cold Spring Harbor Symp. Quant. Biol.* **50**, 643 (1985)]. Color development was clearly visible after 30 min with the MLH1-PMS1 pairwise combination and a positive control, the yeast protein kinase HRR25 [M. F. Hoekstra *et al.*, *Science* **253**, 1031 (1991)] in combination with the HIT1 protein; the other samples were monitored over the next 12 hours. Quantitative assays revealed 5.7 U of β -galactosidase activity for the MLH1-PMS1 combination, 252 U of activity for the positive control, and less than 1 U of activity for all other combinations.
19. The *MLH1* gene was subcloned into an *ADE2*-encoding PG-1 plasmid, which directs high-level constitutive expression in yeast [M. Shena, D. Picard, K. Yamamoto, *Methods Enzymol.* **194**, 389 (1991)]. This construct was transformed into a diploid strain containing the pairwise combination pGAD-MSH2-pBTM-PMS1.
 20. For production of MBP fusion matrices, the *MLH1*, *PMS1*, and *MSH2* genes were cloned into the polylinker of the pMAL-c2 vector (New England Biolabs). Luria broth (500 ml) containing glucose (1 g) and ampicillin (50 mg) was inoculated with 5 ml of an overnight culture of cells expressing the fusion proteins. A crude extract containing MBP fusion proteins was prepared according to the manufacturer's instructions (New England Biolabs). Amylose resin was poured into a 0.7 cm by 15 cm column, and each column was washed with 8 volumes of buffer [20 mM tris HCl (pH 7.4), 200 mM NaCl, 1 mM EDTA, and 1 mM dithiothreitol (DTT)]. The crude extract

was then loaded onto the column, followed by washing with 10 to 12 volumes of buffer.

21. T. A. Prolla, Q. Pang, E. Alani, R. D. Kolodner, R. M. Liskay, data not shown.
22. Plasmids pPY97 and pMQ269 were used to construct homoduplex probes and heteroduplex probes containing a G-T mismatch. The pPY97 plasmid contains the wild-type bacteriophage P22 *mnt* gene [R. T. Sauer *et al.*, *J. Mol. Biol.* **168**, 699 (1983)], and pMQ269 has a T \rightarrow C substitution at position 40. About 50 pmol of two 20-bp oligonucleotides complementary to the *mnt* gene, and 108 bp apart, were treated with T4 kinase (BRL) in the presence of excess ATP. In the polymerase chain reaction (PCR), one of the primers was phosphorylated with T4 kinase and the other was unmodified, depending on which template plasmid (pPY97 or pMQ269) was used. This protocol generates a pair of PCR products, each of which contains a different strand containing a 5' terminal phosphate group. For heteroduplex construction, the double-stranded PCR products generated from pPY97 and pMQ269 were extracted with phenol, precipitated with ethanol, and treated with 5 U of lambda exonuclease (BRL) to degrade the phosphorylated strand of each PCR product. We then generated heteroduplex DNA by annealing single-stranded products from pPY97 and pMQ269 in 1 mM tris HCl (pH 7.5) and 100 mM NaCl. Homoduplex and heteroduplex DNA were labeled with T4 kinase and [γ - 32 P]ATP. For gel retardation assays, MLH1, PMS1, and MSH2 were initially prepared as MBP fusion proteins and were eluted from amylose resin with column buffer con-

taining 10 mM maltose. Factor Xa (New England Biolabs) was added to a final concentration of 20 μ g/ml, and the mixture was incubated at 4°C for 16 hours. The fusion protein cleavage mixture was absorbed on a hydroxyapatite column, and the maltose-free proteins were eluted with 0.5 M sodium phosphate. Proteins were then passed through a second amylose column. The proteins in the flow-through fractions were found to be mostly free of the MBP domain, as determined by SDS-polyacrylamide gel electrophoresis (SDS-PAGE). Proteins were stored at -20°C.

23. J. Jiricny, S.-S. Su, S. G. Wood, P. Modrich, *Nucleic Acids Res.* **16**, 7843 (1988).
24. S. M. Bende and R. H. Grafstrom, *ibid.* **19**, 1549 (1991).
25. P. Modrich, *Annu. Rev. Genet.* **25**, 229 (1991).
26. P. H. von Hippel, *Science* **263**, 769 (1994).
27. A. Sancar and J. E. Hearst, *ibid.* **259**, 1415 (1993).
28. L. T. Haber and G. C. Walker, *EMBO J.* **10**, 2707 (1991).
29. N. C. Nicolaides *et al.*, *Nature*, in press.
30. We thank M. G. Marinus for plasmids pPY97 and pMQ269, M. Hoekstra for the HRR25 and HIT1 positive control plasmids, and M. Thayer and M. Hoekstra for critical comments on the manuscript. Supported by an NSF graduate fellowship (T.A.P.), a Merck fellowship from the Life Sciences Research Foundation (E.A.), NSF grant MCB 9314116 and NIH grants GM 45413 and GM 322741 (R.M.L.), and NIH grant HG00305/GM50006 (R.D.K.).

17 May 1994; accepted 11 July 1994

A Specific Inhibitor of the Epidermal Growth Factor Receptor Tyrosine Kinase

David W. Fry,* Alan J. Kraker, Amy McMichael, Linda A. Ambroso, James M. Nelson, Wilbur R. Leopold, Richard W. Connors, Alexander J. Bridges

A small molecule called PD 153035 inhibited the epidermal growth factor (EGF) receptor tyrosine kinase with a 5-pM inhibition constant. The inhibitor was specific for the EGF receptor tyrosine kinase and inhibited other purified tyrosine kinases only at micromolar or higher concentrations. PD 153035 rapidly suppressed autophosphorylation of the EGF receptor at low nanomolar concentrations in fibroblasts or in human epidermoid carcinoma cells and selectively blocked EGF-mediated cellular processes including mitogenesis, early gene expression, and oncogenic transformation. PD 153035 demonstrates an increase in potency over that of other tyrosine kinase inhibitors of four to five orders of magnitude for inhibition of isolated EGF receptor tyrosine kinase and three to four orders of magnitude for inhibition of cellular phosphorylation.

The EGF receptor is a 170-kD plasma membrane glycoprotein possessing an extracellular ligand-binding domain, a single transmembrane region, and an intracellular domain that exhibits protein tyrosine kinase activity (1). Ligand binding to the EGF receptor results in activation of the kinase activity and leads to autophosphorylation on at least five tyrosines located in the COOH-terminal tail region (2). These initial events are followed by tyrosine phos-

phorylation of various protein substrates, leading to a myriad of signaling and cellular activities (3).

Overexpression of the EGF receptor or its ligands, EGF and transforming growth factor- α , can produce a neoplastic phenotype in cells (4) and transgenic mice (5). Monoclonal antibodies or antisera that block the function of the EGF receptor cause tumor regression in mice bearing human A-431 epidermoid, SW948 colorectal, or nasopharyngeal carcinomas (6). A correlation between the amount of EGF receptor expression in clinical tumor isolates and poor prognosis or short survival time has been established in patients with breast

cancer (7), squamous cell carcinoma of the lung and oral cavity (8), bladder carcinoma (9), and esophageal cancer (10). For these reasons, inhibitors of the EGF receptor tyrosine kinase are potentially useful as chemotherapeutic agents for the treatment of cancer (11).

The molecule PD 153035 was synthesized as one of a series of compounds evaluated as tyrosine kinase inhibitors (Fig. 1). PD 153035 inhibited the EGF receptor tyrosine kinase by 50% at a concentration of 29 ± 5.1 pM (Fig. 2). Because PD 153035 inhibits the reaction at concentrations comparable to those of the enzyme itself, conventional steady-state Michaelis-Menten analysis to determine the inhibition constants (K_i) is inappropriate. The K_i value, therefore, was calculated by nonlinear regression analysis of the equations developed by Morrison (12) for evaluation of tight binding inhibitors and was estimated at 5.2 ± 1.2 pM ($n = 4$). Other less potent analogs of PD 153035, with which steady-state analysis was possible, showed competitive inhibition with respect to adenosine

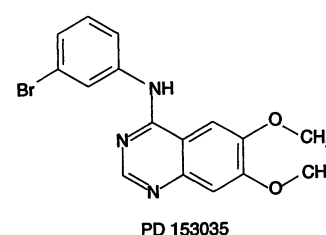


Fig. 1. Chemical structure of PD 153035.

Parke-Davis Pharmaceutical Research, Division of Warner-Lambert Company, 2800 Plymouth Road, Ann Arbor, MI 48105, USA.

*To whom correspondence should be addressed.